https://doi.org/10.1016/j.intermet.2016.05.001

Reliability of the plastic deformation behavior of a Zr-based bulk metallic glass

J.J. Fan[1,#], Y.F. Yan[2,#], S.H. Chen[3,#,*], Chi-Ho Ng[3], F.F., Wu[3,4], and K.C. Chan[3]

[1]School of Mechanical and Electrical Engineering, Hohai University, Changzhou, 213022, China

[2]School of Mechanical Engineering, Anhui University of Technology, Ma'anshan 243002, People's Republic of China

[3]Advanced Manufacturing Technology Research Centre, Department of Industrial and Systems Engineering, The Hong Kong Polytechnic University, Hung Hom, Kowloon, Hong Kong.

[4]School of Materials Science and Engineering, Liaoning University of Technology, Jinzhou, 121001, China.

[#]These authors contributed equally to this work.

*Corresponding author. E-mail: s-h.chen@polyu.edu.hk, cshunhua@gmail.com

Abstract

It is important to interpret the scattering of the plastic deformation behavior data for the structural-applications of bulk metallic glasses (BMGs), however, few studies have focused on statistical analysis of the variation and reliability of the plastic deformation behavior of BMGs. In this work, statistical analyses show unavoidable large variations in the maximum nominal strains of as-cast BMGs, although they exhibited greatly-enhanced average values of the maximum nominal strains with

reduced sample sizes and in the presence of stress gradients. The large variations are attributed to the intrinsic variability of the atomic arrangements stemming from the solidification processes. Nevertheless, the investigations show enhanced cut-off nominal strains (safety threshold) in the specimens with stress gradients. The findings suggest that, despite large variations in the plastic deformation behavior, BMGs are still reliable in practical structural-applications where the materials always deform under more complex stress states.

Key words: A. metallic glasses; B. mechanical properties; B. shear band.

1. Introduction

Due to the non-ordered atomic arrangement, bulk metallic glasses (BMGs) have a number of well-known unique properties, such as an elastic limit of about 2%, high corrosion resistance, high processing ability at higher temperatures and relatively higher strength and hardness compared to their crystalline counterparts [1-5]. As a novel class of structural materials, BMGs have been developed for several decades and are now poised for widespread engineering applications [6-8]. In practical structural-applications of BMGs, they always have a wide range of product dimensions and deform under complex stress states [4,9-14]. It well known that reduced sample sizes [15-21] and the presence of stress gradients [22-24] can enhance the plastic deformation behavior of BMGs. However, due to the metastable atomic arrangements stemming from the solidification processes, the mechanical properties of BMGs demonstrate a wide range of variation. For example, the fracture toughness of BMGs varies significantly from specimen to specimen [25-28]. Since the plastic deformation behavior of BMGs is greatly affected by intrinsic micro-inhomogeneities [29-32], there may also be significant scatter. Understanding the variation of the mechanical properties is vital for the development of structural materials [25,33], and many attempts have been made to investigate the variation of the fracture toughness [25-28] and strength [34-38] of BMGs. Although it is also important to interpret the scattering of plastic deformation behavior data of BMGs in order to avoid catastrophic failures, unfortunately, most of the research so far has focused on how to improve the plastic deformation behavior. Statistical analysis on the variation and the reliability of

the plastic deformation behavior of BMGs has rarely been reported. In this work, the variation of the plastic deformation behavior of a Zr-based BMG with varying sample sizes and stress gradients has been investigated using a large number of specimens, and the corresponding safety thresholds (cut-off nominal strains) have been examined.

2. Experimental

As-cast $Zr_{57}Cu_{20}Al_{10}Ni_8Ti_5$ (at%) BMG rods, with dimensions Φ3 mm × 85 mm and Φ2 mm × 35 mm respectively, were fabricated from pure elements by suction casting the melted ingots into water-cooled copper moulds. The amorphous atomic structures of the as-cast rods were confirmed using standard X-ray diffraction (XRD) analysis. Three groups of specimens were cut from the as-cast rods, as shown in Fig. 1a. Wu et al. [34] reported that the tilting of the samples away from the loading direction can significantly affect the plastic deformation behavior of BMGs. In this work, to minimize the effect of the tilting of the samples, a fixture was used to make sure that all the samples were orthogonal, and the two ends of the specimens were parallel before testing. The orthogonal shapes of the specimens were evidenced by the optical images before the compressive testing (Fig. 1b), and the scanning electron microscopy (SEM) images after testing (Fig. 1c) showed that the phenomenon of tilting away from the loading direction, as discussed in Ref. [34], does not occur. In group III, a tilt angle of 2° (± 0.2°) was tailored at one end surface of the specimens. Under compressive loading, the tilt angle between the end surface of the specimen and the loading platen can result in the presence of a stress gradient to improve the

plastic deformation behavior [22,23]. Room-temperature compression tests were carried out on a servo-hydraulic 810 Material Test System (MTS) at a strain rate of 1 × 10^{-4} s^{-1}, and the nominal strains were recorded using a model 632.13F-20 MTS extensometer. In order to ensure reliable statistical analysis, the specimen number of each group was determined by the equation:

$$n = \left[\frac{Z_{\alpha/2}\delta}{|X-\mu|}\right]^2 \quad (1)$$

where μ and δ^2 are the mean and variance of a population, and $|X-\mu|$ is the estimated maximum error between an individual measurement and the mean. With a confidence level of 100(1−α), $Z_{\alpha/2}$ is the upper α/2 percentage point of the standard normal distribution. In the case of a confidence level of 95% (α=0.05, $Z_{\alpha/2}$=1.645), the minimum specimen number n should in the range 20~30, provided that $\delta/|X-\mu|$ is around 2.5~3.5 which is normally acceptable in reliability engineering [39]. In this work, as confirmed by Ref. [36], 23 specimens for each group were tested for statistical analysis.

3. Results and discussion

Figure 2a shows typical compressive stress-strain curves of the three groups of specimens. It can be seen that for the specimen 3 mm in diameter, the BMG show a limited plasticity of about 2% (group I). The other two groups of specimens, with smaller sample sizes (group II) and stress gradient (group III), demonstrate enhanced nominal plasticity, agreeing well with previous findings [16,21,23]. However, when a large number of specimens are considered, it is found that the maximum nominal

strains display large variations (Fig. 2b). Despite the specimens with smaller sample sizes and the presence of stress gradients having better plastic deformation behavior, they still exhibit wide ranges of maximum nominal strains, differing from the high strength uniformity under compression tests [34,36]. The Weibull distribution has been widely used to evaluate the reliability of samples in safety engineering, and has also been used to characterize the variation of the strength of brittle materials, including BMGs [34-38]. Considering that the nominal strain is proportional to the failure time of the test specimens, the Weibull distribution has also been used to investigate the variation of the maximum nominal strains in this work. The cumulative distribution of the maximum nominal strains of a three-parameter Weibull distribution is given as

$$P_{\mathrm{f}} = 1 - \exp\left[-\left(\frac{\varepsilon - \varepsilon_{\mu}}{\varepsilon_0}\right)^m\right] \qquad (2)$$

where P_{f} is the failure probability for a given nominal strain ε, ε_0 is a scaling parameter and m the Weibull modulus. The parameter ε_{u} is the cut-off nominal strain, denoting the value at which failure will not occur. Eq. (2) was then linearized to obtain the cut-off values of ε_{u}, as shown in the following expression:

$$\ln\left[\ln\left(\frac{1}{1-P_{\mathrm{f}}}\right)\right] = m\ln\left(\varepsilon - \varepsilon_{\mu}\right) - m\ln(\varepsilon_0) \qquad (3)$$

Figure 3 gives the three-parameter Weibull statistical results of the maximum nominal strains, where the Weibull moduli (m) are given in Table 1. As compared with the relatively-larger Weibull moduli of the strength of some Zr-based BMGs (5.98-6.80 [36]), the distributions of the maximum nominal strains have Weibull moduli ranging from 0.92 to 1.21. The small Weibull moduli indicate large variations in the maximum

nominal strains, and the data are right-skewed, where the majority of the specimens are closer to the cut-off values, as shown in Fig. 3b. These findings suggest that although a decrease in the sample sizes and the presence of stress gradients can usually enhance the maximum nominal strain, more attention should be paid to the scattering of the plastic deformation behavior before widespread structural-applications of BMGs.

For a certain alloy composition and the same production processes, the variations of the plastic deformation behavior may result from the variations of the cooling rates at different locations in the as-cast rods. On the one hand, the different locations of the as-cast specimens have different cooling rates during the solidification process, resulting in different plastic deformation behavior [40]. On the other hand, the as-cast specimens also demonstrate different cooling rates between the surfaces and the centre [41,42]. The variation of cooling rates can result in differences in the atomic arrangements [40,42,43] as well as the distribution of the free volume [44]. It is known that BMGs accommodate plastic deformation through the formation and propagation of shear bands [1,5]. The formation of shear bands is significantly affected by the activation of the shear transformation zones (STZs) [45], which are clusters of atoms that are collectively rearrangable under applied stress and preferentially occur at regions with more free volume [46,47]. Thus, the variations in the atomic arrangements, as well as the distributions of the free volume, resulting from the differences in the cooling rates, may be the main cause for the differences in

the maximum nominal strains. Moreover, casting defects may also result in differences in the plastic deformation behavior by influencing the activation of the shear bands [38,45]. The variable atomic arrangements as well as the casting defects, stemming from the solidification processes, can be regarded as intrinsic to BMGs and are unavoidable during the casting processes.

In the application of structural materials, the cut-off nominal strains are always used to denote the safety threshold. In this work, the cut-off values (ε_u) of the three groups of specimens are also given in Table 1. The cut-off value of 2.11% in group I indicates brittle fracture behavior of such a group of specimens. Although the average value of the maximum nominal strains of group II specimens increases by 5.59% as compared with group I specimens, the cut-off nominal strain does not increase significantly (0.47%). Therefore, a decrease in sample size may not be able to avoid catastrophic failures or to mitigate the variations in the plastic deformation behavior when a large number of BMG specimens are involved. (It should be mentioned that the size effect here only refers to the BMG specimens larger than the critical values, below which the stress states and deformation mechanisms are changed during testing [17,20,48]. For example, Volkert et al. [17] have reported the change in the deformation mechanisms from shear-banding-mediated deformation to homogeneous deformation when the sample column diameters decreased to 140 nm in amorphous $Pd_{77}Si_{23}$.) This might be because the increase of the maximum nominal strains in group II is due to changes in the physical nature of the specimens, such as the increase of cooling rates

[41,42] and fewer casting defects [38,45], which intrinsically have large variations. In contrast, group III specimens have a cut-off value of 4.61%, which is relatively larger than the values in groups I (2.11%) and II (2.58%). In the light of the elastic strains of such BMGs, the improvement of the cut-off nominal strain of 2.5% is important in forming a plastic-flow stage to avoid catastrophic failures, resulting in improvement of the reliability in practical applications.

In group III, the increase of the cut-off nominal strain may be attributed to the extrinsically applied stress gradients. Based on an ideal elastic-plastic constitutive model [11], finite element modelling (FEM) analysis was used to characterize the stress distribution of the specimens in group III. At a nominal strain of 2.5%, the FEM results show that yielding only occurs in part of the specimen (Fig. 4a), which is in line with the nominal stress-strain curve in Fig. 2a. It can be seen that the group III specimen has an apparent elastic strain of about 2.5%, which is slightly larger than the values of about 2.25% in groups I and II (Fig. 2a). At the apparent elastic limit (2.5%) of the group III specimen, since the specimen has only partially yielded (Fig. 4a), the nominal stress is smaller than in groups I and II. The stress gradient in group III specimens can also result in a decrease in the apparent elastic modulus, where smaller loads were achieved under the same axial displacements. After the apparent elastic stage, the nominal strain increases continuously to form a work-hardening-like stage up to a strain of about 4.61%, and then fails after a steady stage of plastic flow. Since the ultimate strength of the specimen in group III is no smaller than the value in group

I, a work-hardening-like stage of plastic flow must occur before catastrophic failure. At the cut-off nominal strain 4.61% (Fig. 4b), yielding occurs in almost the whole of the specimen, similar to the yield specimens in group I. At strains larger than the cut-off value, the percentage of the volume and flaws experiencing failure stress in group III specimens may also be similar to the specimens in group I. Therefore, the large variation of the maximum nominal strains in group III, which are larger than the cut-off value, may also be caused by intrinsic variability stemming from the solidification process. It can then be concluded that the increase of the cut-off nominal strain in group III was mainly due to the work-hardening-like plastic-flow stage resulting from the stress gradient, while the large variation of the maximum nominal strains was the result of the intrinsic variability of BMGs.

As a novel class of structural materials, it is important to reduce the variations of the mechanical properties of BMGs in practical applications. The intrinsic variability in the maximum nominal strains cause many uncertainties and unavoidable catastrophic failures, as displayed in the specimens in groups I and II, which are undesirable in industry. Narayan et al. [28] have also observed intrinsical variability of the model I fracture toughness of BMGs. Due to the metastable atomic arrangements stemming from the solidification processes, it is difficult to control the atomic packing and the free-volume distribution accurately. Although attempts have been made to reduce the variations of fracture toughness by thermoplastic-forming the specimens [25], reducing the intrinsic variations of the mechanical properties of BMGs is still very

challenging. Fortunately, the present findings show that although it is difficult to reduce intrinsic uncertainties, their catastrophic failures can be avoided and they are still reliable by introducing stress gradients extrinsically to improve the cut-off nominal strains, as shown in group III. It is known that in practical structural-applications, BMGs always deform under more complex stress states, rather than uniformly distributed stresses or simple stress gradients [4,9-13]. With greatly-improved plastic deformation behavior under complex stress states [49-54], the cut-off nominal strains may be further improved in practical applications. Therefore, despite intrinsic variations, BMGs still possess great potential for structural applications.

4. Conclusions

In summary, the variation and reliability of the plastic deformation behavior of a Zr-based BMG have been examined. Large variations were observed in the maximum nominal strains with the three-parameter Weibull moduli ranging from 0.92 to 1.21, which mainly resulted from the intrinsic variability of the atomic arrangements stemming from the solidification processes. Our further investigations on the cut-off nominal strains revealed that by changing the physical nature of BMGs through reducing the sample sizes, the safety threshold (cut-off nominal strain) was slightly enhanced from 2.11% to 2.58%, however, when an extrinsically stress gradient was introduced, the value was improved to 4.61% by forming a work-hardening-like plastic-flow stage. The findings suggest that, despite intrinsic variability in the plastic

deformation behavior, BMGs are still reliable in practical structural-applications where the materials always deform under more complex stress states.

Acknowledgements

The work described in the paper was partially supported by the Natural Science Foundation of Jiangsu Province (No. BK20150249), Changzhou Sci & Tech Program (No. CJ20159053) and the Fundamental Research Funds for the Central Universities (No. 2014B16014). FFW appreciates the financial support from the National Natural Science Foundation of China (NSFC) under Grant No 51571106, the Liaoning BaiQianWan Talents Program (Grant No. 2014921056), the Natural Science Foundation of Liaoning Province (Grant No. 2015020244), and the Program for Liaoning Excellent Talents in University (Grant No. LJQ2014064).

References

[1] A.R. Yavari, J.J. Lewandowski, J. Eckert, Mechanical properties of bulk metallic glasses, MRS Bull. 32 (2007) 635-638.

[2] W.H. Wang, Bulk metallic glasses with functional physical properties, Adv. Mater. 21 (2009) 4524-4544.

[3] A.L. Greer, Metallic glasses ... on the threshold, Mater. Today 12 (2009) 14-22.

[4] J. Schroers, Processing of bulk metallic glass, Adv. Mater. 22 (2010) 1566-1597.

[5] M.M. Trexler, N.N. Thadhani, Mechanical properties of bulk metallic glasses, Prog. Mater. Sci. 55 (2010) 759-839.

[6] M.F. Ashby, A.L. Greer, Metallic glasses as structural materials, Scripta Mater. 54 (2006) 321-326.

[7] J. Plummer, W.L. Johnson, Is metallic glass poised to come of age?, Nat. Mater. 14 (2015) 553-555.

[8] A. Inoue, F.L. Kong, S.L. Zhu, E. Shalaan, F.M. Al-Marzouki, Production methods and properties of engineering glassy alloys and composites, Intermetallics 58 (2015) 20-30.

[9] G. Kumar, A. Desai, J. Schroers, Bulk metallic glass: The smaller the better, Adv. Mater. 23 (2011) 461-476.

[10] S.H. Chen, K.C. Chan, F.F. Wu, L. Xia, Pronounced energy absorption capacity of cellular bulk metallic glasses, Appl. Phys. Lett. 104 (2014) 111907.

[11] S.H. Chen, K.C. Chan, L. Xia, Deformation behavior of bulk metallic glass structural elements, Mater. Sci. Eng. A 606 (2014) 196-204.

[12] E.R. Homer, M.B. Harris, S.A. Zirbel, J.A. Kolodziejska, H. Kozachkov, B.P. Trease, J.P.C. Borgonia, G.S. Agnes, L.L. Howell, D.C. Hofmann, New methods for developing and manufacturing compliant mechanisms utilizing bulk metallic glass, Adv. Eng. Mater. 16 (2014) 850-856.

[13] S.H. Chen, K.C. Chan, F.F. Wu, L. Xia, Achieving high energy absorption capacity in cellular bulk metallic glasses, Sci. Rep. 5 (2015) 10302.

[14] S.H. Chen, K.C. Chan, G. Wang, J. Yi, Saw-tooth-like bulk metallic glass structures with greatly enhanced energy-absorption performance, J. Alloys Compd. 661 (2016) 49-54.

[15] Y. Wu, H.X. Li, Z.B. Jiao, J.E. Gao, Z.P. Lu, Size effects on the compressive deformation behaviour of a brittle Fe-based bulk metallic glass, Phil. Mag. Lett. 90 (2010) 403-412.

[16] N. Li, Q. Chen, L. Liu, Size dependent plasticity of a Zr-based bulk metallic glass during room temperature compression, J. Alloys Compd. 493 (2010) 142-147.

[17] C.A. Volkert, A. Donohue, F. Spaepen, Effect of sample size on deformation in amorphous metals, J. Appl. Phys. 103 (2008) 083539.

[18] Y.J. Huang, J. Shen, J.F. Sun, Bulk metallic glasses: Smaller is softer, Appl. Phys. Lett. 90 (2007) 081919.

[19] J. Yi, W.H. Wang, J.J. Lewandowski, Sample size and preparation effects on the tensile ductility of Pd-based metallic glass nanowires, Acta Mater. 87 (2015) 1-7.

[20] F.F. Wu, Z.F. Zhang, S.X. Mao, Size-dependent shear fracture and global tensile plasticity of metallic glasses, Acta Mater. 57 (2009) 257-266.

[21] F.F. Wu, Z.F. Zhang, S.X. Mao, J. Eckert, Effect of sample size on ductility of metallic glass, Phil. Mag. Lett. 89 (2009) 178-184.

[22] L.Y. Chen, Q. Ge, S. Qu, Q.K. Jiang, X.P. Nie, J.Z. Jiang, Achieving large macroscopic compressive plastic deformation and work-hardening-like behavior in a monolithic bulk metallic glass by tailoring stress distribution, Appl. Phys. Lett. 92 (2008) 211905.

[23] W.F. Wu, C.Y. Zhang, Y.W. Zhang, K.Y. Zeng, Y. Li, Stress gradient enhanced plasticity in a monolithic bulk metallic glass, Intermetallics 16 (2008) 1190-1198.

[24] S.H. Chen, K.C. Chan, L. Xia, Effect of stress gradient on the deformation

behavior of a bulk metallic glass under uniaxial tension, Mater. Sci. Eng. A 574 (2013) 262-265.

[25] W. Chen, J. Ketkaew, Z. Liu, R.M.O. Mota, K. O'Brien, C.S. da Silva, J. Schroers, Does the fracture toughness of bulk metallic glasses scatter?, Scripta Mater. 107 (2015) 1-4.

[26] C.P. Kim, J.Y. Suh, A. Wiest, M.L. Lind, R.D. Conner, W.L. Johnson, Fracture toughness study of new Zr-based Be-bearing bulk metallic glasses, Scripta Mater. 60 (2009) 80-83.

[27] J.H. Schneibel, J.A. Horton, P.R. Munroe, Fracture toughness, fracture morphology, and crack-tip plastic zone of a Zr-based bulk amorphous alloy, Metall. Mater. Trans. A 32 (2001) 2819-2825.

[28] R.L. Narayan, P. Tandaiya, G.R. Garrett, M.D. Demetriou, U. Ramamurty, On the variability in fracture toughness of ‘ductile’ bulk metallic glasses, Scripta Mater. 102 (2015) 75-78.

[29] J. Das, M.B. Tang, K.B. Kim, R. Theissmann, F. Baier, W.H. Wang, J. Eckert, "Work-hardenable" ductile bulk metallic glass, Phys. Rev. Lett. 94 (2005) 205501.

[30] G. Wang, Y.H. Liu, P. Yu, D.Q. Zhao, M.X. Pan, W.H. Wang, Structural evolution in TiCu-based bulk metallic glass with large compressive plasticity, Appl. Phys. Lett. 89 (2006) 251909.

[31] A. Makino, X. Li, K. Yubuta, C.T. Chang, T. Kubota, A. Inoue, The effect of Cu on the plasticity of Fe-Si-B-P-based bulk metallic glass, Scripta Mater. 60 (2009) 277-280.

[32] J.M. Park, J.H. Na, D.H. Kim, K.B. Kim, N. Mattern, U. Kuhn, J. Eckert, Medium range ordering and its effect on plasticity of Fe-Mn-B-Y-Nb bulk metallic glass, Philos. Mag. 90 (2010) 2619-2633.

[33] J.M. Torralba, F. Velasco, J.M. RuizRoman, L.E.G. Cambronero, J.M. RuizPrieto, Reliability and homogeneity study of sintered steels through the Weibull statistic, J. Mater. Sci. Lett. 15 (1996) 2105-2107.

[34] W.F. Wu, Y. Li, C.A. Schuh, Strength, plasticity and brittleness of bulk metallic glasses under compression: statistical and geometric effects, Philos. Mag. 88 (2008) 71-89.

[35] J.H. Yao, J.Q. Wang, L. Lu, Y. Li, High tensile strength reliability in a bulk metallic glass, Appl. Phys. Lett. 92 (2008) 041905.

[36] Z. Han, L.C. Tang, J. Xu, Y. Li, A three-parameter Weibull statistical analysis of the strength variation of bulk metallic glasses, Scripta Mater. 61 (2009) 923-926.

[37] P. Jia, Z.D. Zhu, X.W. Zuo, E.G. Wang, J.C. He, Investigations of compressive strength on Cu-Hf-Al bulk metallic glasses: Compositional dependence of malleability and Weibull statistics, Intermetallics 19 (2011) 1902-1907.

[38] C.J. Lee, Y.H. Lai, J.C. Huang, X.H. Du, L. Wang, T.G. Nieh, Strength variation and cast defect distribution in metallic glasses, Scripta Mater. 63 (2010) 105-108.

[39] K.C. Kapur, M. Pecht, Reliability Engineering, John Wiley & Sons., 2014.

[40] J. Shen, Y.J. Huang, J.F. Sun, Plasticity of a TiCu-based bulk metallic glass: Effect of cooling rate, J. Mater. Res. 22 (2007) 3067-3074.

[41] Q.S. Zhang, W. Zhang, X.M. Wang, Y. Yokoyama, K. Yubuta, A. Inoue, Structure,

thermal stability and mechanical properties of Zr(65)Al(7.5)Ni(10)Cu(17.5) glassy alloy rod with a diameter of 16 mm produced by tilt casting, Mater. Trans. 49 (2008) 2141-2146.

[42] S.H. Chen, D. Ding, P. Yu, Z.W. Wang, L. Xia, Hierarchical amorphous structures in a $Zr_{50}Cu_{42}Al_8$ bulk metallic glass, Mater. Sci. Eng. A 639 (2015) 75-79.

[43] J. Das, S. Pauly, C. Duhamel, B.C. Wei, J. Eckert, Microstructure and mechanical properties of slowly cooled $Cu_{47.5}Zr_{47.5}Al_5$, J. Mater. Res. 22 (2007) 326-333.

[44] L.Y. Chen, A.D. Setyawan, H. Kato, A. Inoue, G.Q. Zhang, J. Saida, X.D. Wang, Q.P. Cao, J.Z. Jiang, Free-volume-induced enhancement of plasticity in a monolithic bulk metallic glass at room temperature, Scripta Mater. 59 (2008) 75-78.

[45] A.L. Greer, Y.Q. Cheng, E. Ma, Shear bands in metallic glasses, Mater. Sci. Eng. R 74 (2013) 71-132.

[46] L. Li, E.R. Homer, C.A. Schuh, Shear transformation zone dynamics model for metallic glasses incorporating free volume as a state variable, Acta Mater. 61 (2013) 3347-3359.

[47] A. Bhattacharyya, G. Singh, K.E. Prasad, R. Narasimhan, U. Ramamurty, On the strain rate sensitivity of plastic flow in metallic glasses, Mater. Sci. Eng. A 625 (2015) 245-251.

[48] C.Q. Chen, Y.T. Pei, J.T.M. De Hosson, Effects of size on the mechanical response of metallic glasses investigated through in situ TEM bending and compression experiments, Acta Mater. 58 (2010) 189-200.

[49] Z.T. Wang, J. Pan, Y. Li, C.A. Schuh, Densification and strain hardening of a

metallic glass under tension at room temperature, Phys. Rev. Lett., 111 (2013) 135504.

[50] C.E. Packard, C.A. Schuh, Initiation of shear bands near a stress concentration in metallic glass, Acta Mater. 55 (2007) 5348-5358.

[51] S. Jana, U. Ramamurty, K. Chattopadhyay, Y. Kawamura, Subsurface deformation during Vickers indentation of bulk metallic glasses, Mater. Sci. Eng. A 375 (2004) 1191-1195.

[52] S.H. Chen, K.C. Chan, L. Xia, Deformation behavior of a Zr-based bulk metallic glass under a complex stress state, Intermetallics 43 (2013) 38-44.

[53] F.F. Wu, Z.F. Zhang, J. Shen, S.X. Mao, Shear deformation and plasticity of metallic glass under multiaxial loading, Acta Mater. 56 (2008) 894-904.

[54] S.H. Chen, K.C. Chan, G. Wang, F.F. Wu, L. Xia, J.L. Ren, J. Li, K.A. Dahmen, P.K. Liaw, Loading-rate-independent delay of catastrophic avalanches in a bulk metallic glass, Sci. Rep. 6 (2016) 21967.

Figure captions

Figure 1. (a) Schematic diagram of the three groups of BMG specimens. (b) Optical images showing the specimens before compressive testing. (c) SEM images showing three specimens at fracture, where ε is the nominal strain at failure.

Figure 2. Compressive testing results of the three groups of specimens, where (a) shows three typical stress-strain curves, and (b) shows the distribution of the maximum nominal strains of 23 specimens. The data in (b) were distributed as the increase of the maximum nominal strains, and the inset shows a magnified view.

Figure 3. Three-parameter Weibull plots of the maximum nominal strains (a), where (b) is the corresponding density distribution.

Figure 4. FEM results showing the stress distributions of the group III specimens at nominal strains of 2.5% (a) and 4.61% (b) respectively.

Table 1. The statistical results of the maximum nominal strains of the specimens, where N is the number of specimens, ε_a is the average value and ε_s the standard deviation of the maximum nominal strain. m and ε_u are the three-parameter Weibull modulus and the cut-off nominal strain, respectively.

Group	N	ε_a (%)	ε_s (%)	Minimum (%)	Median (%)	Maximum (%)	m	ε_u (%)
I	23	4.29	2.01	2.27	3.76	11.50	1.21	2.11
II	23	9.88	5.55	2.66	7.85	21.80	1.14	2.58
III	23	8.09	4.56	4.72	6.50	26.05	0.92	4.61

Figure 1

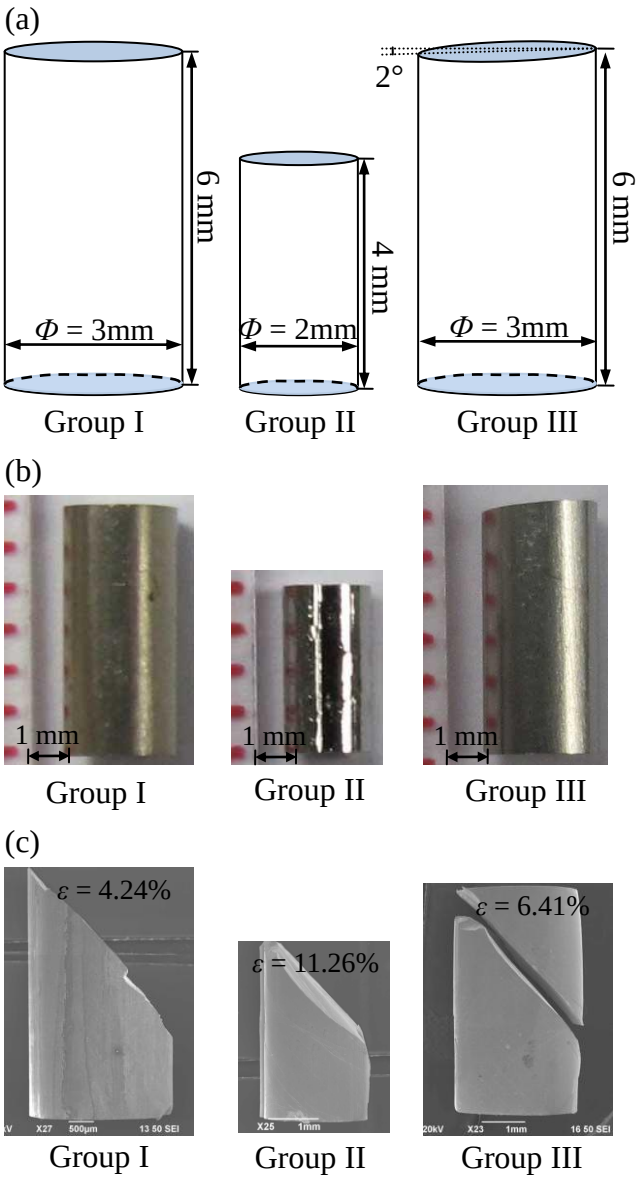

J.J. Fan *et al*.

Fig. 1

Figure 2

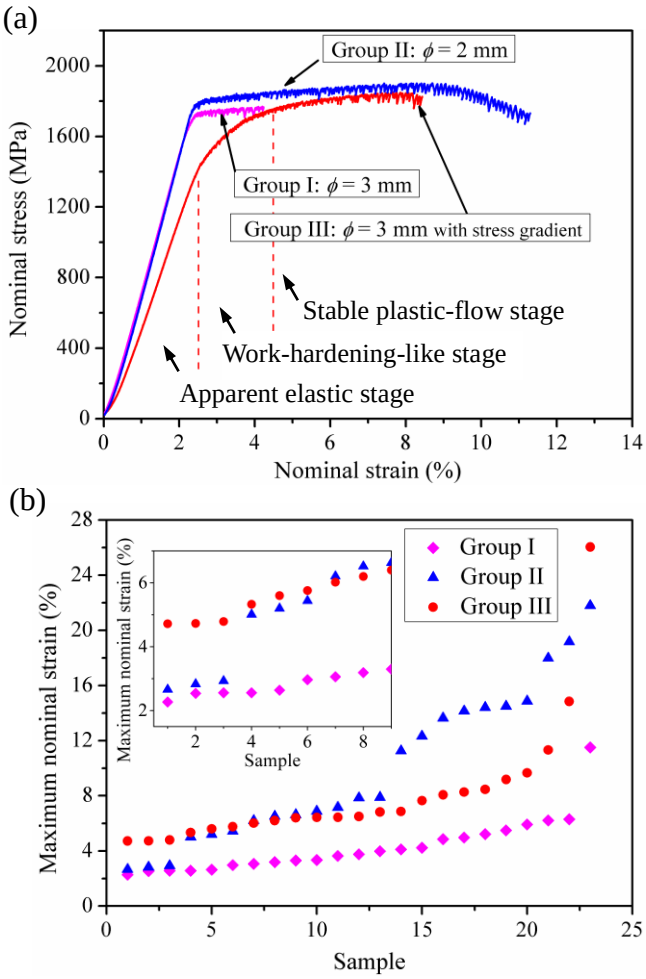

J.J. Fan *et al.*

Fig. 2

Figure 3

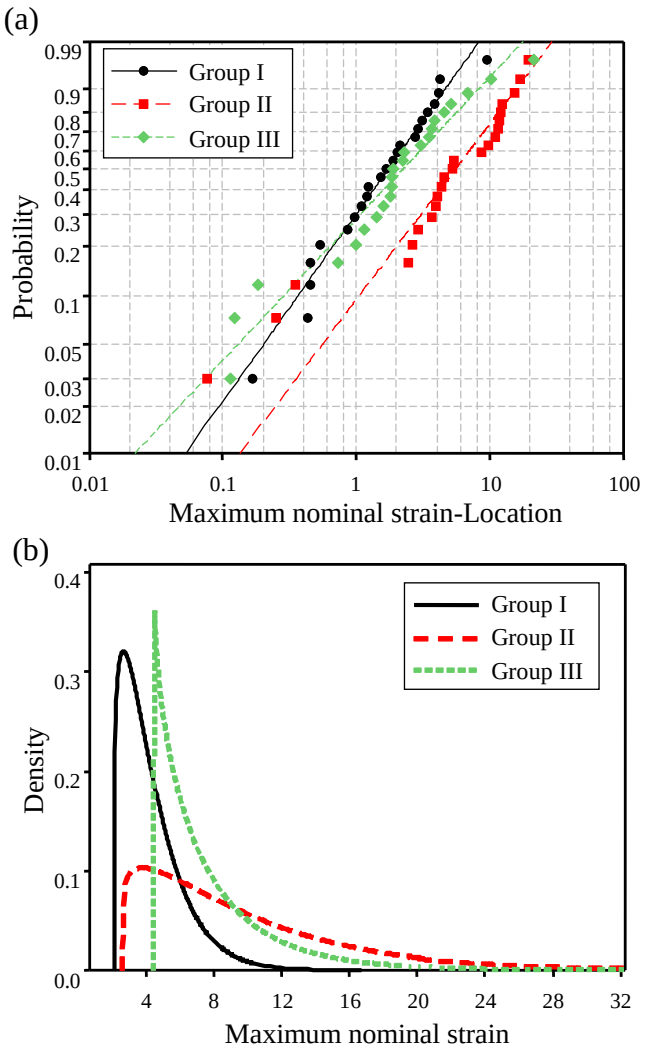

J.J. Fan *et al.*

Fig. 3

Figure 4

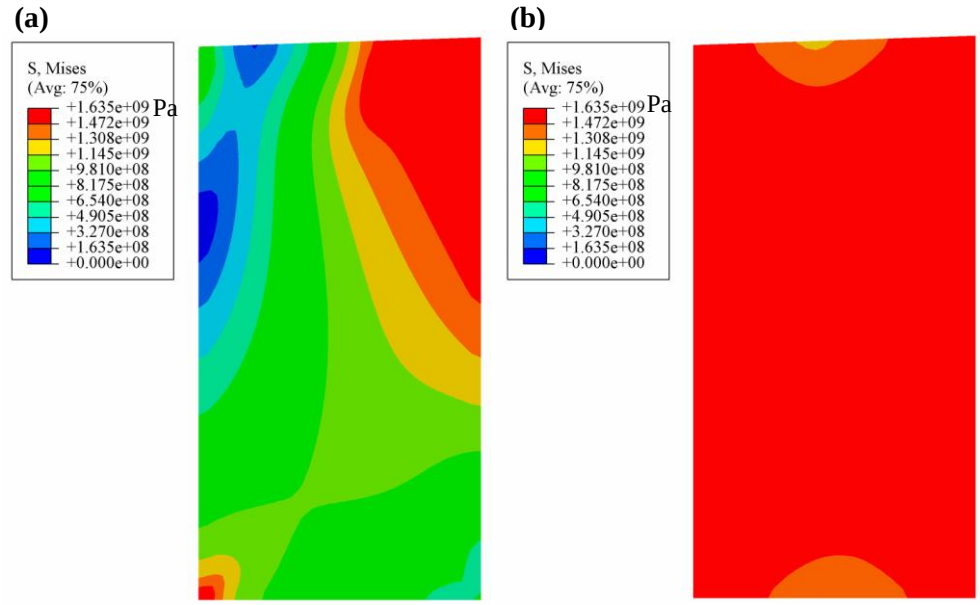

J.J. Fan *et al.*

Fig. 4